Electronic Supplementary Material (ESI) for Analytical Methods.

Pd-Pt-Ru nanozyme with peroxidase-like activity for the detection of total antioxidant capacity

Jian He[a], Lin Yang[a], Ying Zhang[d], Ranhui Li[b], Jingjun Wu[a], Qianqian Cao[a], Sang Li[a],Xian Wu[c], Yunfeng Duan[c], Dongxiu He[a]* Weiguo Wang[a]*

a Institute of Pharmacy and Pharmacology, University of South China, HengYang 421000, Hunan, China; Hunan Province Cooperative Innovation Center for Molecular Target New Drug Study, Hengyang, Hunan, China; Hunan Xinhexin Biological Medicine Co., Ltd. Pharmacy Graduate Education Innovation Base

b Institute of Pathogenic Biology, Hengyang Medical School, University of South China, Hengyang, 421000, Hunan, China.

c The First Affiliated Hospital of Hunan College of Traditional Chinese Medicine, Hunan Province Directly Affiliated TCM Hospital, Zhuzhou, China.

d School of Biomedical and Chemical Engineering, Liaoning Institute of Science and Technology, Benxi, 117004, China.

** Corresponding author.*

E-mail: 1025165380@qq.com (Dongxiu He)

wang901234@163.com (Weiguo Wang)

1.Materials

Potassium chloroplatinate (K_2PtCl_6,98%), potassium tetrabromopalladium (K_2PdBr_4, 98%), sodium hexachloroiridate hydrate ($RuCl_3$), Pluronic F127, ascorbic acid (AA, 99%), glutathione (GSH), cysteine (Cys), potassium bromide (KBr, 99%), poly (vinyl pyrrolidone) (PVP, MW≈55,000) and ethylene glycol (EG, 99%), 3,3',5,5'-tetramethylbenzidine (TMB), were all ordered from Aladdin. The UV-visible absorption spectra were obtained from Lambda 265 (PerkinElmer, United States). Transmission electron microscopy (TEM) images were obtained from FEL talos F200s (Thermo Fisher Scientific, United States), and scanning electron microscopy (SEM) pictures were acquired by using Sigma 500 (Zeiss, Britain). X-ray photoelectron spectroscopy (XPS) was recorded by Thermo ESCALAB 250XI (Thermo Fisher Scientific, United States).

2. Methods

2.1Fluorescent detection of OH radical

Terephthalic acid is highly selective and react with hydroxyl radicals to generate 2-hydroxy terephthalic acid which emits unique fluorescence around 450 nm. In this test, 10 μL of PPR nanozyme solution was added to 2.5 mL of acetic acid buffer solution (HAC-NaAC pH=4) cotaining 100 μL of TA (0.05mM) and 400 μL H_2O_2 (62.5mM). Finally, the fluorescence spectra of the samples were collected after 30 minutes of reaction by fluorescence spectroscopy.

2.2The detection of hydrogen peroxide

For the detection of hydrogen peroxide, 400 μL of samples with different concentrations of H_2O_2 (0-40mM) were added into the mixed solution of 2.5 mL HAc-NaAc buffer (pH=4,), TMB (100 μL, 0.02mM, dissolved in DMSO) and Pd-Pt-Ru (10 μL). The mixture was immediately scanned using UV-vis spectrometer.

2.3The detection of AA

For the detection of AA, 20 μL of varied concentrations of AA was mingled into 2.5 mL of HAc-NaAc buffer (pH=4) containing 62.5 mM of H_2O_2, PPR nanozyme of 10 μL, 100 μL of TMB (0.02mM), dissolved in DMSO), followed by rapidly stirring. After the reaction, the absorption variation at 652 nm was measured via a UV-vis spectrophotometer, and the absorption peaks were employed for the quantitative determination of AA.

2.4 TAC assay

Taking AA as a typical model, the TAC of several herbs and food (*Fructus Corni*, *Radix Paeoniae Alba*, *Rhizoma Dioscoreae Bulbiferae* and *Folium Eriobotryae*, tomato, orange, green tea, Ice tea and Lemon) were measured. The concentrations of real samples were diluted to avoid exceeding the linear range of AA detection. The TAC test was evaluated under the same condition as the AA test, but with real sample instead of AA. The absorbances of ox-TMB were brought into the standard curve. Then the value of TAC was obtained through absorbance conversion.

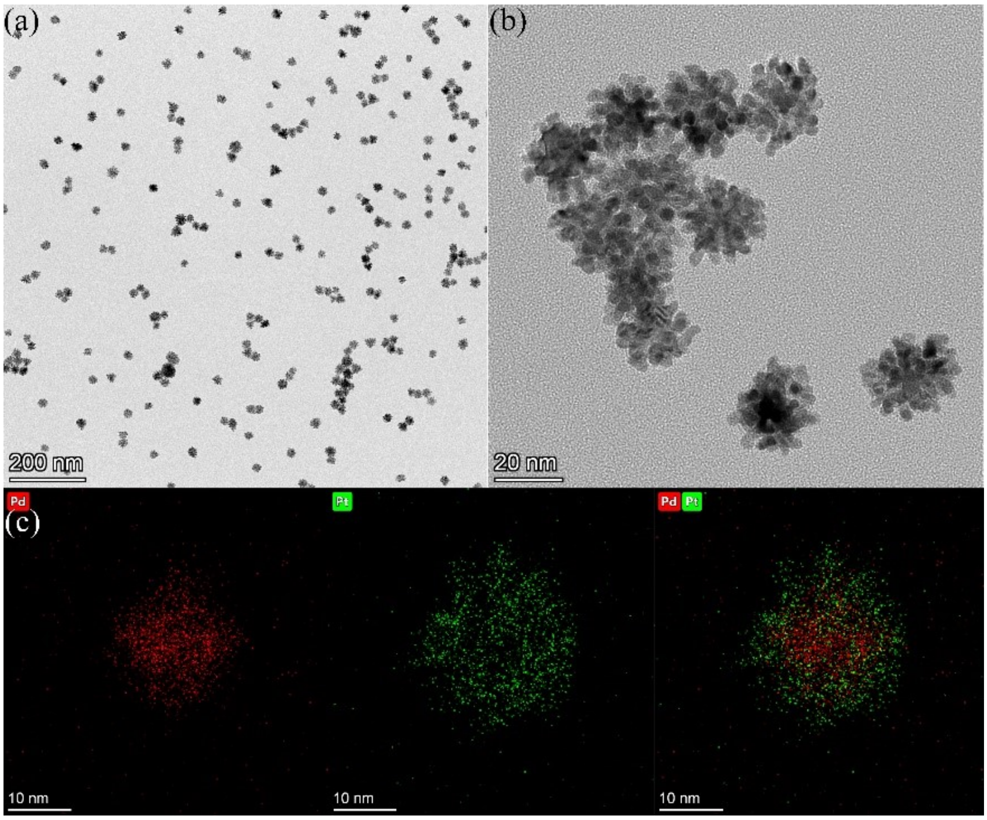

Figure S1 (a) the TEM of Pd-Pt nanoparticles;(b) the HRTEM pattern of Pd-Pt nanoparticles; (c) element distribution of Pd-Pt nanoparticles.

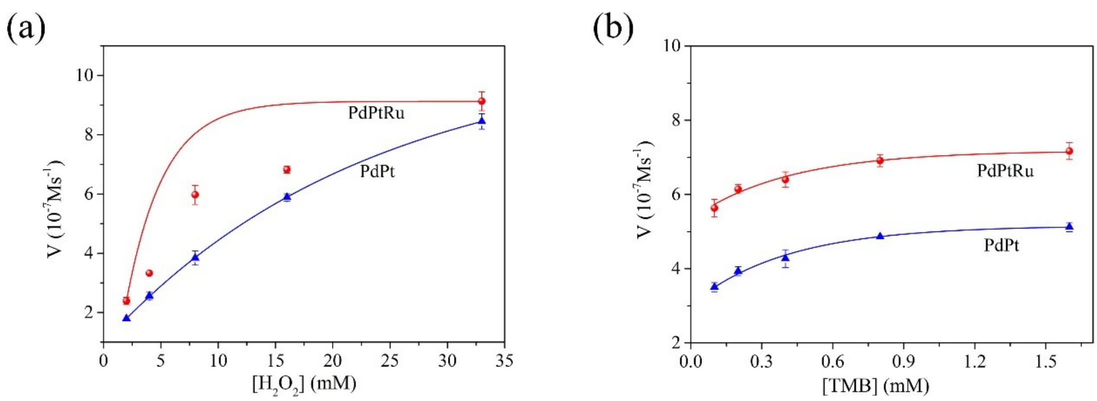

Figure S2 The velocity (v) of the reaction changes in the presence of different concentrations of (a) H_2O_2 and (b)TMB.

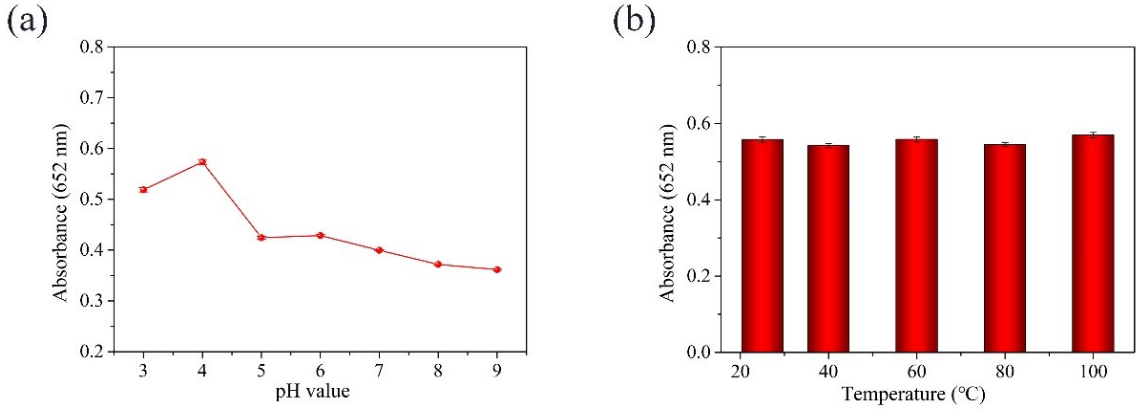

Figure S3 the stability test of Pd-Pt-Ru nanozyme (a) pH and (b) temperature.

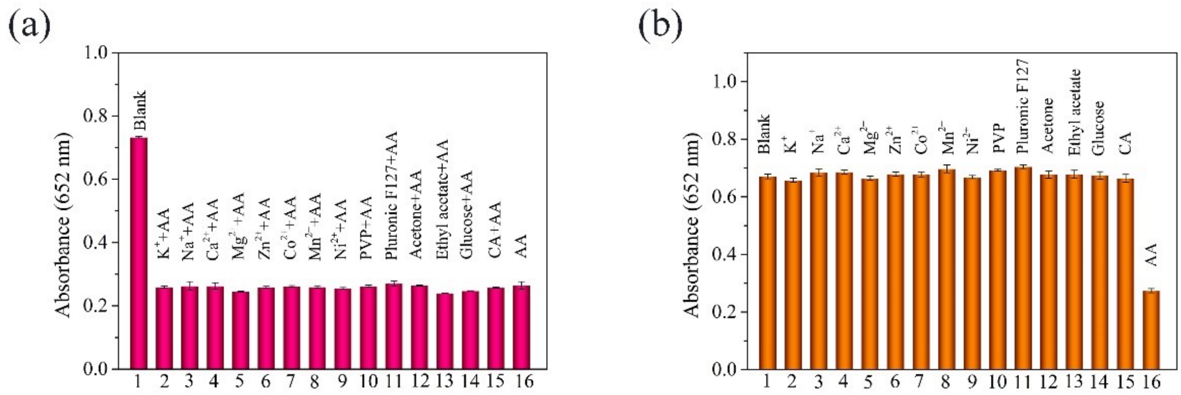

Figure S4 the evaluation of (a) interference resistance and (b) specificity

Table S1 Comparison of kinetic parameters of different catalysts

Catalyst	Substrate	K_m(mM)	V_{max}(MS^{-1})	Referrence
PPR	H_2O_2	6.64	10.00×10^{-7}	This work
	TMB	0.026	7.07×10^{-7}	
Pd-Pt	H_2O_2	7.53	8.20×10^{-7}	This work
	TMB	0.047	5.02×10^{-7}	
Citrate-Pt NPs	H_2O_2	205.6	9.79×10^{-8}	[1]
	TMB	0.1206	6.51×10^{-8}	
Chitosan-Pd NPs	H_2O_2	537.71	1.12×10^{-7}	[2]
	TMB	0.09	1.77×10^{-7}	
Ru NPs	H_2O_2	2.206	5.83×10^{-7}	[3]
	TMB	0.234	8.25×10^{-8}	
HRP	H_2O_2	3.7	8.71×10^{-8}	[4]
	TMB	0.434	10×10^{-8}	
Fe_3O_4	H_2O_2	154	9.78×10^{-8}	[4]
	TMB	0.098	3.44×10^{-8}	

Table S2 Comparison of various materials and methods used in AA biosensors.

Catalyst	Linear range	Detection limit	Reference
$CuMnO_2$ nanoflowers	1-105 μM	0.39 μM	[10]
Cu nanoclusters	0.5-30 μM	0.144 μM	[11]
Fe–Mn nanozyme	8-56 μM	0.88 μM	[12]
GA-Ag nanozyme	0.03-0.14 mM	3.0 μM	[13]
Pt–Ni alloy	0.57-5.7 mM	0.33 mM	[14]
Au/Cu NRs	0-2 mM	25 μM	[15]
PdIr aerogels	0.5-250 μM	0.22 μM	[16]
NCNTs@MoS2	0.2-80μM	0.12μM	[17]
SNC nanozyme	0.1-5 mM	0.08 mM	[18]
PPR nanozyme	2-12 μM	1.13μM	This work

[1] G. W. Wu, S. B. He, H. P. Peng, Citrate-capped platinum nanoparticle as a smart probe for ultrasensitive mercury sensing, *Analytical Chemistry*. 2014; 86: 10955-10960.

[2] P. Meiling, T. Wang, Z. Z. Jiang, Surfactant-Free synthesis of PdPt/rGO for the alkaline ethanol oxidation reaction, *Nano*; 2017; 12: 1750105.

[3] G. J. Cao, X. M. Jiang, H. Zhang, T. R. Croley, J. J. Yin, Mimicking horseradish peroxidase and oxidase using ruthenium nanomaterial, *RSC Advances.* 2017; 7: 52210-52217.

[4] H. Wei, E. K. Wang, Fe_3O_4 magnetic nanoparticles as peroxidase mimetics and their applications in H_2O_2 and glucose detection, *Analytical Chemistry.* 2008; 80: 2250–2254.

[5] Q. Lian, X.F. Zheng, G.R Peng, Z.Q. Liu, L. Chen, S. Wu, Oxidase mimicking of $CuMnO_2$ nanoflowers and the application in colorimetric detection of ascorbic acid, *Colloids and Surfaces A: Physicochemical and Engineering Aspects*. 2022; 652.

[6] C.Y. Liu, Y.Y. Cai, J. Wang, X. Liu, L. Yan, Y.J. Zhang, S.Q. Yang, J. Guo, Facile preparation of homogeneous copper nanoclusters exhibiting excellent tetraenzyme mimetic activities for colorimetric glutathione sensing and fluorimetric ascorbic acid Sensing, *ACS Applied Materials Interfaces.* 2020; 12: 42521-42530.

[7] Y. Han, L.P. Luo, L. Zhang, H. Sun, J. Dan, W.T. Zhang, T. L. Yue, J. L Wang, Oxidase-like Fe–Mn bimetallic nanozymes for colorimetric detection of ascorbic acid in kiwi fruit, *LWT - Food Science and Technology.* 2022;154.

[8] V. D. Doan, V. C. Nguyen, T. H. Nguyen, A. T. Nguyen, T. D. Nguyen, Highly sensitive and low-cost colourimetric detection of glucose and ascorbic acid based on silver nanozyme biosynthesized by Gleditsia australis fruit, *Spectrochimica*

Acta PartA: Molecular and Biomolecular Spectroscopy. 2022; 268.

[9] Y. C. Weng, Y. G. Lee, Y. L. Hsiao, C. Y. Lin, A highly sensitive ascorbic acid sensor using a Ni–Pt electrode, *Electrochim Acta*. 2011; 56: 9937-9945.

[10] S. Y. Xu, X. J. Dong, S. Q. Chen, Y. Y. Zhao, G. Y. Shan, Y. C. Sun, Y. C. Liu, The preparation of high-index facet Au/Cu NRs and their application for colorimetric determination ascorbic acid, *Sensors and Actuators B-Chemistry.* 2019; 281: 375-382.

[11] X. Tan, Q. Yang, X. Sun, P. Sun, H. Li, PdIr Aerogels with boosted peroxidase-like activity for a sensitive total antioxidant capacity colorimetric bioassay, *ACS Applied Materials Interfaces*. 2022; 14: 10047-10054.

[12] J. Zheng, D. D. Song, H. Chen, J. L. Xu, N. S. Alharbi, T. Hayat, M. Zhang, Enhanced peroxidase-like activity of hierarchical MoS_2-decorated N-doped carbon nanotubes with synergetic effect for colorimetric detection of H_2O_2 and ascorbic acid, *Chinese Chemical Letters*. 2020; 31: 1109-1113.

[13] Y. Chen, L. Jiao, H. Yan, W. Xu, Y. Wu, H. Wang, Hierarchically porous S/N codoped carbon nanozymes with enhanced peroxidase-like activity for total antioxidant capacity, *Biosensing Analytical Chemistry*. 2020; 92: 13518-13524.